

## POLYNOMIAL FITTING FOR EDGE DETECTION IN IRREGULARLY SAMPLED SIGNALS AND IMAGES\*

RICK ARCHIBALD<sup>†</sup>, ANNE GELB<sup>‡</sup>, AND JUNGHO YOON<sup>§</sup>

**Abstract.** We propose a new edge detection method that is effective on multivariate irregular data in any domain. The method is based on a local polynomial annihilation technique and can be characterized by its convergence to zero for any value away from discontinuities. The method is numerically cost efficient and entirely independent of any specific shape or complexity of boundaries. Application of the *minmod* function to the edge detection method of various orders ensures a high rate of convergence away from the discontinuities while reducing the inherent oscillations near the discontinuities. It further enables distinction of jump discontinuities from steep gradients, even in instances where only sparse nonuniform data is available. These results are successfully demonstrated in both one and two dimensions.

**Key words.** *minmod* function, multivariate edge detection, Newton divided differencing, non-uniform grids

**AMS subject classifications.** 41A25, 41A45, 41A63

**DOI.** 10.1137/S0036142903435259

**1. Introduction.** Edge detection is of fundamental importance in image analysis. In particular, a reliable and efficient edge detection method can both provide the possibility of processing an image with high accuracy as well as serve to simplify the analysis of images by drastically reducing the amount of data to be processed. Among the many common criteria relevant to edge detector performance, there are two very important issues. The first and most obvious issue is the possibility of failing to find real edge points and/or falsely identifying nonedge points. Regardless of specific types of data (regular or irregular) and domains, it is imperative that the edges occurring in the image should not be missed, and that there be no spurious responses. This is critical since the edges of the image constitute piecewise smooth regions. Hence errors in edge identification could also have drastic consequences on image reconstruction. The second issue is the necessity for simple implementation and cost efficiency.

To address these issues, this study constructs an edge detection method based on local Taylor expansions. Indeed, several well-known methods exist in the univariate case (see, e.g., [2], [3], [4], [5], [11], and the references therein). However, for the bivariate case, particularly with irregular points, no successful method has thus far been developed. Recent developments (see [1] and [15]) in essentially nonoscillatory (ENO) and weighted essentially nonoscillatory (WENO) methods for hyperbolic conservation laws and Hamilton–Jacobi equations on multidimensional unstructured meshes also utilize Taylor expansions to determine regions of analyticity. For uniform sampling,

---

\*Received by the editors August 28, 2003; accepted for publication (in revised form) September 3, 2004; published electronically May 27, 2005. This research was supported in part by NSF grants CNS 0324957, DMS 0107428, EAR 0222327, and KRF-2002-070-C00014.

<http://www.siam.org/journals/sinum/43-1/43525.html>

<sup>†</sup>Department of Neuroscience, Brown Medical School, Box 1953, Providence, RI 02912 (Richard.Archibald@brown.edu). The research of this author was supported in part by the SSERC.

<sup>‡</sup>Department of Mathematics and Statistics, Arizona State University, Tempe, Arizona 85287-1804 (ag@math.la.asu.edu). The research of this author was supported in part by NIH grant EB 02533-01.

<sup>§</sup>Department of Mathematics, Ewha W. University, Seoul, 120-750, South Korea (yoon@math.ewha.ac.kr).

we note that while ENO and WENO methods identify stencils yielding the “most” smooth polynomial interpolations, they do not distinguish between, say, steep gradients and edges. In our method, Taylor expansions are used for the exclusive purpose of determining the true edges of an image by incorporating various orders and stencil sizes.

In this paper we present an edge detection method for multivariate irregular data that has the following desirable properties: (I) It can be applied to any irregular data in any domain. (II) It is independent of any specific shape of discontinuities in both the univariate and bivariate cases. (III) The method depends only on locally sampled signals, making it easy to implement numerically, since for each point our scheme needs only to solve a simple matrix and no global system of equations needs to be solved. (IV) It has a fast rate of convergence to zero away from the discontinuities. The benefit of the last property is that the edge detection method will be able to distinguish jumps from steep gradients more readily than methods of slower convergence. There will be additional considerations, as it will become apparent that high order edge detection methods produce more oscillations in the neighborhoods of the jump discontinuities. To distinguish true jump locations from neighborhood oscillations, we find from [13] that the *minmod* function (see Definition 3.1), typically used for reducing oscillations in the presence of shocks in numerical solutions for conservation laws (see, e.g., [7]), may help to reduce oscillations in the presence of jump discontinuities. We extend this idea to our edge detection method for the case of multivariate irregular data and moreover provide a proof for its convergence rate to zero away from the discontinuities, which has previously not been accomplished.

This study is primarily concerned with the detection of jump discontinuities (or fault detection). While it is important to consider the effects of a noisy environment on an edge detection method, it is beyond the scope of this introductory paper. Hence we leave the study of noise for future investigations.

This paper is organized as follows: In section 2 we present the formulation of the edge detection method. In section 3 we use this formulation to construct an edge detection method for the one-dimensional case and employ the *minmod* function to the edge detection method. Section 4 is devoted to analyzing the behavior of the edge detection method in two dimensions. Finally, some numerical algorithms are provided in Appendices A and B.

**2. General formulation for edge detection.** Let us first introduce the following notation, which will be used throughout this paper:

For  $x = (x_1, \dots, x_d)$  in  $\mathbb{R}^d$ ,  $|x| := (x_1^2 + x_2^2 + \dots + x_d^2)^{1/2}$  stands for its Euclidean norm. For any finite set of points  $\mathcal{S}$  in  $\mathbb{R}^d$  we use the notation  $K_{\mathcal{S}}$  for the convex hull of the set  $\mathcal{S}$ . We denote by  $\mathbb{N} := \{1, 2, \dots\}$  the set of natural numbers and by  $\mathbb{Z}_+ := \{0, 1, 2, \dots\}$  the set of nonnegative integers. For any  $\alpha \in \{(\alpha_1, \dots, \alpha_d) : \alpha_1, \dots, \alpha_d \in \mathbb{Z}_+\} := \mathbb{Z}_+^d$ , we set  $|\alpha|_1 := \sum_{k=1}^d \alpha_k$ , and  $\alpha! := \alpha_1! \cdots \alpha_d!$ . Throughout  $\alpha$  is a multivariate nonnegative integer that will change dimension based upon the dimension under discussion. We denote a uniform grid of density  $h$  as  $h\mathbb{Z}^d := \{h\alpha \mid \alpha \in \mathbb{Z}^d\}$ . We use the usual notation  $\lceil s \rceil$  to indicate the smallest integer greater than or equal to  $s$ . For any  $m \in \mathbb{Z}_+$ ,  $\Pi_m$  denotes the space of all polynomials of degree  $\leq m$  in  $d \in \mathbb{N}$  variables where the dimension of  $\Pi_m$  is denoted by

$$(2.1) \quad m_d := \binom{m+d}{d}.$$

We recall the Dirac delta function

$$(2.2) \quad \delta_{i,j} = \begin{cases} 1 & \text{if } i = j, \\ 0 & \text{if } i \neq j. \end{cases}$$

Finally, throughout this paper we use  $A$  to represent an arbitrary constant that may change value.

We introduce an edge detection method on the set of irregularly distributed points in a bounded domain  $\Omega$  in  $\mathbb{R}^d$ . Let  $\mathcal{S}$  be a set of discrete points in  $\Omega$  and let  $f$  be a piecewise smooth function known only on  $\mathcal{S}$ . In order to identify the jump discontinuities of  $f$ , we construct a function  $L_m f$ ,  $m \in \mathbb{N}$ , which can be characterized by the asymptotical convergence property,

$$L_m f(x) \longrightarrow 0,$$

for any  $x$  away from discontinuities, with the convergence rate depending in part on the given positive integer  $m$ . The choice of  $m$  is user dependent, but a higher number  $m$  provides a faster rate of convergence in smooth regions of  $f$ .

The edge detection method presented here is based on a local polynomial annihilation property. The general form of  $L_m f$  is given by the following two step method. In the first step, for any  $x \in \Omega$ , we choose a set

$$(2.3) \quad \mathcal{S}_x := \mathcal{S}_{m_d, x} := \{x_1, \dots, x_{m_d}\},$$

which is a local set of  $m_d$  (2.1) points around  $x$ . In practice, though the dimension  $d$  can be arbitrary, we consider only the case  $d \leq 2$  and note that for  $d > 2$  the method is the same although the numerical algorithms are more complicated.

In order to annihilate polynomials up to degree  $m - 1$ , we solve a linear system for the coefficients  $c_j(x)$ ,  $j = 1, \dots, m_d$ , given by

$$(2.4) \quad \sum_{x_j \in \mathcal{S}_x} c_j(x) p_i(x_j) = \sum_{|\alpha|_1=m} p_i^{(\alpha)}(x), \quad \alpha \in \mathbb{Z}_+^d,$$

where  $p_i$ ,  $i = 1, \dots, m_d$ , is a basis of  $\Pi_m$ . Note that the solution (2.4) exists and is unique. Our edge detector  $L_m f$  is defined, using the solution of (2.4), as

$$(2.5) \quad L_m f(x) = \frac{1}{q_{m,d}(x)} \sum_{x_j \in \mathcal{S}_x} c_j(x) f(x_j).$$

Here  $q_{m,d}(x)$  is a suitable normalization factor depending on  $m$ , the dimension  $d$ , and the local set  $\mathcal{S}_x$  (2.3). In the following sections, we will determine  $q_{m,d}(x)$  specifically for  $d = 1, 2$ . Indeed, for the univariate case the normalization factor  $q_{m,d}(x)$  is important in detecting the jump amount at a discontinuity. However, in the multivariate case, it is no longer meaningful since the jump amount varies depending on the directions at a discontinuity. In this case  $q_{m,d}(x)$  can be used to estimate the magnitude of the jump in its normal direction, as will be explained later.

It is evident from (2.5) that  $L_m f$  is *local* in the sense that it employs data only in a small neighborhood of  $x$ . It is also apparent that (2.5) detects edges regardless of the geometrical aspects of the discontinuities. Furthermore, we will show that  $L_m f(x)$  converges to zero away from the discontinuities with a certain rate depending on  $m$  and the local smoothness of the function  $f$ .

**3. Edge detection in one dimension.**

**3.1. Formulation.** Throughout section 3, let  $f$  be a piecewise smooth function on an interval  $[a, b]$ , known only at the finite discrete points

$$\mathcal{S} \subset [a, b], \quad \#\mathcal{S} =: N < \infty,$$

which we will call “nodes.” Suppose that  $f$  has jump discontinuities with well-defined one-sided limits, and let

$$J = \{\xi : a \leq \xi \leq b\}$$

denote the set of jump discontinuities of  $f$  in  $[a, b]$ . We define the local jump function corresponding to  $f$  as

$$[f](x) := f(x+) - f(x-),$$

where  $f(x+)$  and  $f(x-)$  are the right- and left-hand limits of the function  $f$  at  $x$ . Clearly, if  $f$  is continuous at  $x$ , then  $[f](x) = 0$  and for any  $\xi \in J$ ,  $[f](\xi) = f(\xi+) - f(\xi-) \neq 0$ .

The ability to find the locations and corresponding amplitudes of the jump discontinuities depends on the accuracy of the approximation to the jump function  $[f](x)$ . Hence we construct  $L_m f(x)$  in (2.5) to be an approximation to  $[f](x)$  such that

$$(3.1) \quad L_m f(x) \longrightarrow \begin{cases} [f](\xi) & \text{if } x_{j-1} \leq \xi, x \leq x_j \text{ for } \xi \in J, \\ 0 & \text{if } I_x \cap J = \emptyset, \end{cases}$$

where  $I_x$  is the smallest closed interval such that  $\mathcal{S}_x \subset I_x$ , with  $\mathcal{S}_x$  defined in (2.3). In this way, a jump discontinuity  $\xi \in J$  is identified by its enclosed cell,  $x_{j-1} \leq \xi \leq x_j$ , and the convergence rate of the approximation  $L_m f(x)$  to the jump function  $[f](x)$  is given in terms of

$$(3.2) \quad h(x) := \max\{|x_i - x_{i-1}| : x_{i-1}, x_i \in \mathcal{S}_x\}.$$

Clearly  $h(x)$  is dependent upon the density of  $\mathcal{S}_x$ .

The function  $L_m f$  for the univariate case is defined as follows: For the given positive integer  $m$ , we choose a local set  $\mathcal{S}_x$  of  $m_1$  points around  $x$ . Here  $m_1$  is the dimension of  $\Pi_m$  in  $\mathbb{R}$  as given by (2.1), i.e.,  $m_1 = m + 1$ . The coefficients utilized in the edge detection method are determined by the solution of the linear system

$$(3.3) \quad \sum_{x_j \in \mathcal{S}_x} c_j(x) p_i(x_j) = p_i^{(m)}(x), \quad i = 1, \dots, m_1,$$

where  $p_i, i = 1, \dots, m_1$ , is a basis of  $\Pi_m$ . Clearly, the coefficients  $c_j(x)$  are uniquely determined by the local set  $\mathcal{S}_x$ , and are of order  $\mathcal{O}(h(x)^{-m})$  as  $h(x) \rightarrow 0$ . Fortunately, an explicit formula exists for  $c_j(x)$  that will be described later in Theorem 3.2.

Next, by defining

$$(3.4) \quad \mathcal{S}_x^+ := \{x_j \in \mathcal{S}_x | x_j \geq x\} \quad \text{and} \quad \mathcal{S}_x^- := \mathcal{S}_x \setminus \mathcal{S}_x^+,$$

we set the normalization factor in (2.5) as

$$(3.5) \quad q_m(x) := q_{m,1}(x) := \sum_{x_j \in \mathcal{S}_x^+} c_j(x),$$

such that  $q_m(x) \neq 0$ . Note from (3.3) that it is clear that  $q_m(x)$  is of order  $\mathcal{O}(h(x)^{-m})$  as well.

Finally, the edge detection method (2.5) in the one-dimensional case is

$$(3.6) \quad L_m f(x) = \frac{1}{q_m(x)} \sum_{x_j \in \mathcal{S}_x} c_j(x) f(x_j).$$

There is no restriction in choosing the sets  $\mathcal{S}_x^+$  and  $\mathcal{S}_x^-$  in (3.4), but from a practical point of view, a good choice is to put almost the same numbers of nodes on each side of  $x$ . For instance, if  $m$  is odd, one may choose  $\mathcal{S}_x^+$  and  $\mathcal{S}_x^-$  such that  $\#\mathcal{S}_x^+ = \#\mathcal{S}_x^-$ . These sets will have to be adjusted near the boundary of the domain, and naturally will become more one-sided.

In order for  $L_m f$  in (3.6) to be successful, it should approximate the jump function  $[f](x)$  with high accuracy. Theorem 3.1 shows that  $L_m f(x)$  converges to zero away from the jump discontinuities of  $f$  with a certain rate depending on  $m$  and the local smoothness of  $f$ .

**THEOREM 3.1.** *Let  $m \in \mathbb{N}$  and  $L_m f(x)$  be defined as in (3.6) using a local set  $\mathcal{S}_x$  with  $\#\mathcal{S}_x = m_1 = m + 1$ . Then we have*

$$L_m f(x) = \begin{cases} [f](\xi) + \mathcal{O}(h(x)) & \text{if } x_{j-1} \leq \xi, x \leq x_j, \\ \mathcal{O}(h^{\min(m,k)}(x)) & \text{if } f \in C^k(I_x) \text{ for } k > 0, \end{cases}$$

where  $h(x)$  is given in (3.2) and  $I_x$  is the smallest closed interval such that  $\mathcal{S}_x \subset I_x$ .

*Proof.* Assume first that  $f \in C^k(I_x)$  for some  $k > 0$ . Denote  $k_m := \min(k, m) > 0$  and let  $T_{k_m-1} f$  be the Taylor expansion of  $f$  of degree  $k_m - 1$  around  $x$ , namely,

$$T_{k_m-1} f(\cdot) = \sum_{\alpha=0}^{k_m-1} (\cdot - x)^\alpha f^{(\alpha)}(x) / \alpha!.$$

Since  $T_{k_m-1} f$  is a polynomial of degree less than  $m$ , the definition of  $c_j(x)$  in (3.3) implies that

$$(3.7) \quad \sum_{x_j \in \mathcal{S}_x} c_j(x) T_{k_m-1} f(x_j) = 0.$$

By rewriting  $f = T_{k_m-1} f + R_{k_m-1} f$ , where  $R_{k_m-1} f$  is the remainder of Taylor expansion, it follows from (3.7) that

$$\begin{aligned} |L_m f(x)| &= \left| \frac{1}{q_m(x)} \sum_{x_j \in \mathcal{S}_x} c_j(x) R_{k_m-1} f(x_j) \right| \\ &= \left| \frac{1}{q_m(x)} \sum_{x_j \in \mathcal{S}_x} c_j(x) (x_j - x)^{k_m} f^{(k_m)}(\zeta_j) / k_m! \right| \\ &\leq Ah^{k_m}(x) \frac{1}{|q_m(x)|} \sum_{x_j \in \mathcal{S}_x} |c_j(x)| \end{aligned}$$

for some  $\zeta_j$  between  $x$  and  $x_j$ , where the last inequality is implied since  $|x - x_j| \leq mh(x)$  for any  $x_j \in \mathcal{S}_x$  and  $|f^{(k_m)}(x) / k_m!|$  is bounded for  $x \in I_x$ . Since both  $c_j(x)$  and  $q_m(x)$  are  $\mathcal{O}(h^{-m}(x))$ , it is clear that  $|L_m f(x)| \leq Ah^{k_m}(x)$ .

Next, consider the case that  $x_{j-1} \leq \xi, x \leq x_j$  for  $\xi \in J$  and  $x_{j-1}, x_j \in \mathcal{S}_x$ . Without loss of generality, assume that  $\xi$  is the only discontinuity of  $f$  in a neighborhood  $I_\xi$  and  $\mathcal{S}_x \subset I_\xi$ . Invoking the notation  $\mathcal{S}_x^+$  and  $\mathcal{S}_x^-$  in (3.4), we have

$$\begin{aligned} L_m f(x) &= \frac{1}{q_m(x)} \sum_{x_j \in \mathcal{S}_x^+} c_j(x) f(x_j) + \frac{1}{q_m(x)} \sum_{x_j \in \mathcal{S}_x^-} c_j(x) f(x_j) \\ &= \frac{1}{q_m(x)} \sum_{x_j \in \mathcal{S}_x^+} c_j(x) [f(\xi^+) + (x_j - \xi) f'(\zeta_j^+)] \\ &\quad + \frac{1}{q_m(x)} \sum_{x_j \in \mathcal{S}_x^-} c_j(x) [f(\xi^-) + (x_j - \xi) f'(\zeta_j^-)] \end{aligned}$$

for some  $\zeta_j^+$  and  $\zeta_j^-$ . Since (2.4) implies that  $\sum_{x_j \in \mathcal{S}_x} c_j(x) = 0$ , it follows that

$$\sum_{x_j \in \mathcal{S}_x^+} c_j(x) = - \sum_{x_j \in \mathcal{S}_x^-} c_j(x).$$

Utilization of (3.5) yields

$$L_m f(x) = (f(\xi^+) - f(\xi^-)) + \mathcal{O}(h(x))$$

to complete the proof.  $\square$

Next, Theorem 3.2 establishes the relationship between the edge detection method (3.6) and Newton divide differences, which are frequently employed to determine smooth regions in finite difference schemes (see, for example, [6], [9], and [12]). This beneficial relationship provides an explicit formula for the coefficients  $c_j(x)$  without solving the linear system (3.3). Denoting  $\mathcal{S}_x =: \{x_1, \dots, x_{m_1}\}$  with  $m_1 = m + 1$ , recall the definition of the  $m_1$ th degree Newton divided difference for a smooth function  $f(x)$  on  $\mathcal{S}_x$ :

$$\begin{aligned} (3.8) \quad f[\mathcal{S}_x] &:= f[x_1, x_2, \dots, x_{m_1}] = \frac{f[x_1, x_2, \dots, x_{m_1-1}] - f[x_2, x_3, \dots, x_{m_1}]}{x_1 - x_{m_1}} \\ &= \sum_{j=1}^{m_1} \frac{f(x_j)}{\omega_j(\mathcal{S}_x)} = \frac{f^{(m)}(\xi)}{m!}, \end{aligned}$$

where  $\xi \in (x_1, x_{m_1})$  and

$$(3.9) \quad \omega_j(\mathcal{S}_x) := \prod_{\substack{i=1 \\ i \neq j}}^{m_1} (x_j - x_i).$$

**THEOREM 3.2.** *Under the same conditions and notation as Theorem 3.1, the coefficients  $c_j(x)$  can be directly solved as*

$$(3.10) \quad c_j(x) = \frac{m!}{\omega_j(\mathcal{S}_x)}, \quad j = 1, \dots, m_1,$$

with  $\omega_j(\mathcal{S}_x)$  in (3.9). Furthermore, the  $L_m f(x)$  in (3.6) can be expressed as

$$L_m f(x) = \frac{m!}{q_m(x)} f[\mathcal{S}_x].$$

*Proof.* Since the coefficients  $c_j(x)$  that solve (3.3) are independent of the basis of  $\Pi_m$ , it is enough to consider the basis  $p_i(x) = x^{i-1}$  for  $i = 1, \dots, m_1$ . The  $m$ th derivative of these basis functions satisfies

$$(3.11) \quad p_i^{(m)}(x) = m! \delta_{i,m_1} \quad \text{for all } x \in \mathbb{R}.$$

By (3.8), it is possible to conclude that  $p_i[\mathcal{S}_x] = \delta_{i,m_1}$ , yielding  $m!p_i[\mathcal{S}_x] = p_i^{(m)}(x)$ ,  $i = 1, \dots, m_1$ . Hence by (3.8) we have

$$m! \sum_{j=1}^{m_1} \frac{p_i(x_j)}{\omega_j(\mathcal{S}_x)} = p_i^{(m)}(x), \quad i = 1, \dots, m_1,$$

indicating that the coefficients  $c_j(x)$  can also be formulated by (3.10).

Given the direct representation (3.10) of the coefficients  $c_j(x)$  as the solution of the linear system (3.3), the edge detection method (3.6) can be expressed as

$$\begin{aligned} L_m f(x) &= \frac{1}{q_m(x)} \sum_{x_j \in \mathcal{S}_x} c_j(x) f(x_j), \\ &= \frac{m!}{q_m(x)} \sum_{x_j \in \mathcal{S}_x} \frac{f(x_j)}{\omega_j(\mathcal{S}_x)} = \frac{m!}{q_m(x)} f[\mathcal{S}_x], \end{aligned}$$

finishing the proof.  $\square$

*Remark 3.1.* Let  $x \in (a, b)$  be fixed and let  $I_x^+$  be the smallest closed interval such that  $\mathcal{S}_x^+ \subset I_x^+$ . Choosing  $f = \chi_{I_x^+}$  with  $\chi_{I_x^+}$  the characteristic function on  $I_x^+$ , Theorem 3.2 implies that the normalization factor  $q_m(x)$  in (3.5) can be written as

$$\begin{aligned} q_m(x) &= \sum_{x_j \in \mathcal{S}_x^+} c_j(x) \\ &= \sum_{x_j \in \mathcal{S}_x} c_j(x) \chi_{I_x^+}(x_j) = m! \chi_{I_x^+}[\mathcal{S}_x]. \end{aligned}$$

Thus, the assumption  $q_m(x) \neq 0$  is reasonable.

*Remark 3.2.* As discussed above, for any given data  $(\mathcal{S}, f|_{\mathcal{S}})$ , the evaluation of  $L_m f(x)$  involves only finite local data  $(\mathcal{S}_x, f|_{\mathcal{S}_x})$  around  $x$ . Accordingly, if  $\mathcal{S}$  is a set of irregular points, the coefficients  $c_j(x)$  may vary depending on the location  $x$ . However, if the given set  $\mathcal{S}$  is uniform, say,

$$(3.12) \quad \mathcal{S} := \{a + nh \mid n = 0, \dots, N\}, \quad h = \frac{b-a}{N} > 0,$$

then there exists only one set of coefficients  $c_j(x) = c_j$ ,  $j = 1, \dots, m_1$ , which are independent of the position  $x$  inside  $[a, b]$  (but away from the boundary). Specifically, (3.10) can be directly applied to obtain the coefficients

$$c_j = \frac{m!}{\omega_j(\mathcal{S}_x)} = \frac{m!}{h \prod_{i=1, i \neq j}^{m_1} (j-i)}, \quad j = 1, \dots, m_1,$$

which in turn yields the normalization factor  $q_m = q_m(x)$  in (3.5). Hence  $\frac{c_j}{q_m}$  in (3.6) is bounded and independent of both  $h$  and  $x$ , and consequently the numerical computation of (3.6) is further simplified, while keeping the same convergence properties in Theorem 3.1.

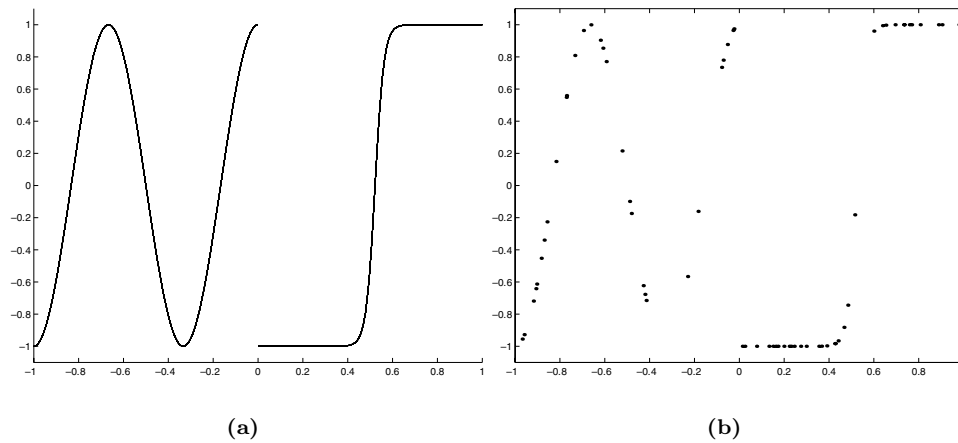


FIG. 3.1. (a) Graph of  $f_1(x)$ . (b) Random sampling of  $f_1(x)$  on  $N = 64$  points.

To demonstrate the efficacy of the edge detection method  $L_m f(x)$ , let us consider the following example.

*Example 3.1.*

$$(3.13) \quad f(x) := \begin{cases} \cos(3\pi x), & -1 \leq x < 0, \\ \frac{2}{1+3e^{-50x+25}} - 1, & 0 < x \leq 1. \end{cases}$$

The function  $f(x)$  has an edge at  $x = 0$  and the corresponding jump function

$$(3.14) \quad [f](x) = \begin{cases} -2 & \text{if } x = 0, \\ 0 & \text{else.} \end{cases}$$

We wish to approximate  $[f](x)$ , based on the scattered grid point values generated randomly by MATLAB and depicted in Figure 3.1(b). Figure 3.2 demonstrates the application of  $L_m f(x)$  for  $m = 1, 3, 4$ , and 6.

Observe in Figure 3.2 that the application of (3.6) encounters some problems in the approximation of jump functions. Specifically, as  $m$  increases, oscillations that occur in the neighborhood of a jump discontinuity can be misidentified as true edges. On the other hand, for smaller  $m$ , there is a risk of identifying a steep gradient as an edge, especially in regions where the scattered grid points are far apart. We wish to avoid the possibility of misidentification due either to the low resolution problems associated with the low order edge detection or to the oscillations inherent in the high order case. Presented in the following section is the *minmod* edge detection method that helps to prevent the edge detection method (3.6) from misidentifying edges.

**3.2. Minmod edge detection in one dimension.** It was observed in [13] that the *minmod* function, typically used in numerical conservation laws to reduce oscillations (see, e.g., [7]), could also be applied to distinguish true jump discontinuities from neighborhood oscillations. In what follows we describe the oscillating behavior near the jump discontinuities that results from using our local edge detector (3.6). Thus motivated, we extend the use of the *minmod* function and incorporate various orders of  $m$  for nonuniform grids. Moreover, we provide the proof of its convergence rate to zero away from the discontinuities. We will refer to this technique as the *minmod* edge detection method.



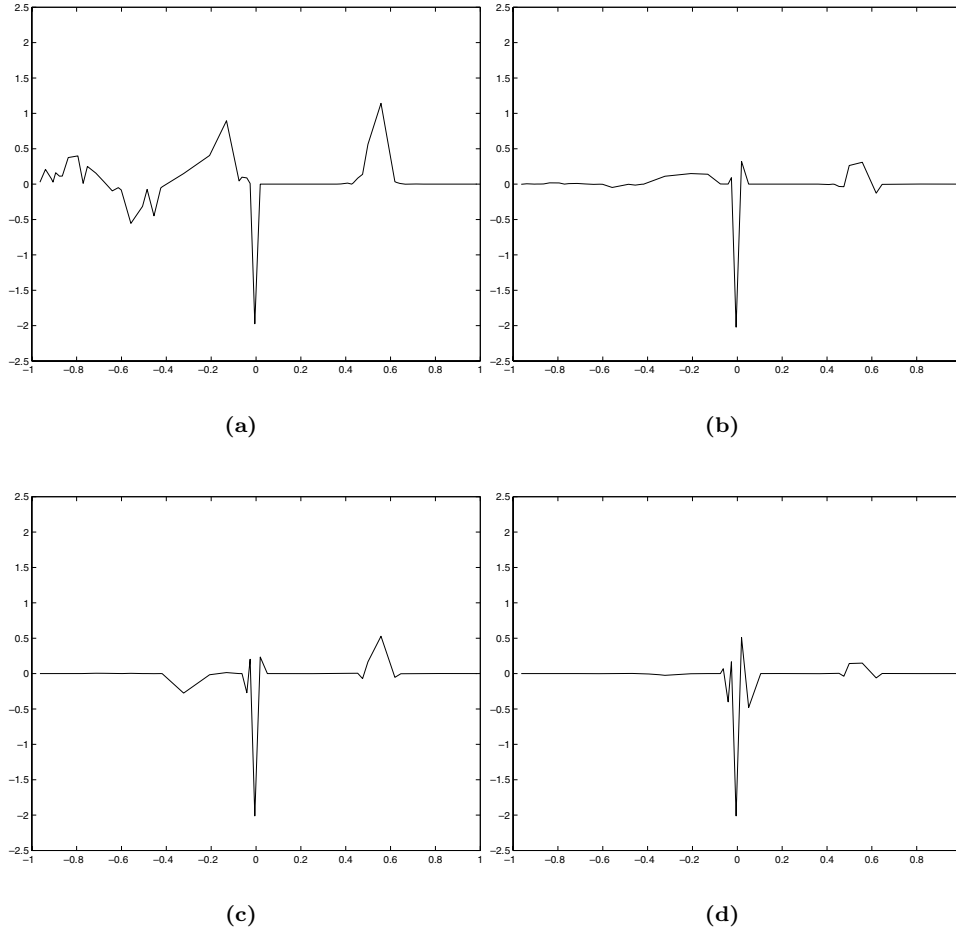


FIG. 3.2. The edge detection method  $L_m f(x)$  given by (3.6) for (a)  $m = 1$ , (b)  $m = 3$ , (c)  $m = 4$ , and (d)  $m = 6$ .

The next theorem describes the behavior of the edge detection method (3.6) in the neighborhoods of discontinuities and motivates the need for further refinement by the *minmod* function.

**THEOREM 3.3.** Let  $m \in \mathbb{N}$  and  $L_m f(x)$  be defined as in (3.6) using  $\mathcal{S}_x$  with  $\#\mathcal{S}_x = m_1$ , and let

$$(3.15) \quad Q_m(\xi, x) := \sum_{x_j \in \mathcal{S}_\xi^+} c_j(x)$$

with  $\mathcal{S}_\xi^+ := \{x_j \in \mathcal{S}_x \mid x_j \geq \xi\}$  as given in (3.4). Then

$$L_m f(x) = \begin{cases} \frac{Q_m(\xi, x)}{q_m(x)} [f](\xi) + \mathcal{O}(h(x)) & \text{if } I_x \cap \xi \neq \emptyset \text{ for } \xi \in J, \\ \mathcal{O}(h^{\min(m,k)}(x)) & \text{if } f \in C^k(I_x) \text{ for } k > 0. \end{cases}$$

Here,  $I_x$  is the smallest closed interval such that the local set  $\mathcal{S}_x \subset I_x$ .

*Proof.* Assume first that  $I_x \cap J = \emptyset$  and therefore  $f \in C^k(I_x)$  for some  $k > 0$ . It is therefore possible to conclude by Theorem 3.1 that  $L_m f(x) = \mathcal{O}(h^{\min(m,k)}(x))$ .

Next, let us consider the case that  $I_x \cap J \neq \emptyset$ . Without loss of generality, assume that  $\xi$  is the only discontinuity of  $f$  in a neighborhood  $I_x$ . Invoking the notation  $\mathcal{S}_\xi^+$  and  $\mathcal{S}_\xi^-$  in (3.4), we see that

$$\begin{aligned} L_m f(x) &= \frac{1}{q_m(x)} \sum_{x_j \in \mathcal{S}_\xi^+} c_j(x) f(x_j) + \frac{1}{q_m(x)} \sum_{x_j \in \mathcal{S}_\xi^-} c_j(x) f(x_j) \\ &= \frac{1}{q_m(x)} \sum_{x_j \in \mathcal{S}_\xi^+} c_j(x) [f(\xi^+) + (x_j - \xi) f'(\zeta_j)] \\ &\quad + \frac{1}{q_m(x)} \sum_{x_j \in \mathcal{S}_\xi^-} c_j(x) [f(\xi^-) + (x_j - \xi) f'(\zeta_j)] \end{aligned}$$

with  $\zeta_j$  between  $x_j$  and  $\xi$ . Here, from the condition  $\sum_{x_j \in \mathcal{S}_x} c_j(x) = 0$  in (3.3), it is clear that

$$Q_m(\xi, x) := \sum_{j \in \mathcal{S}_\xi^+} c_j(x) = - \sum_{j \in \mathcal{S}_\xi^-} c_j(x).$$

Hence

$$L_m f(x) = \frac{Q_m(\xi, x)}{q_m(x)} (f(\xi^+) - f(\xi^-)) + \mathcal{O}(h(x)),$$

which completes the proof.  $\square$

The behavior characterized in Theorem 3.3 is visible in Figure 3.2 as  $m$  increases in (3.6). Specifically, the edge detection method approximates the jump function with high order outside the neighborhoods of the discontinuities. Unfortunately, inside the neighborhoods of the discontinuities the edge detection method oscillates according to the fraction  $\frac{Q_m(\xi, x)}{q_m(x)} [f](\xi)$ .

The *minmod* edge detection method, as defined below, uses the *minmod* function to exploit the characteristics of the edge detection method of various orders both inside and outside the neighborhoods of the discontinuities to ensure the highest order of convergence possible away from the discontinuity, as well as to reduce the oscillations inside the neighborhoods of discontinuities.

DEFINITION 3.1. For a given finite set  $\mathcal{M} \subset \mathbb{N}$  of positive integers, consider the set  $L_{\mathcal{M}} f = \{L_m f : \mathbb{R} \rightarrow \mathbb{R} \mid m \in \mathcal{M}\}$ . The *minmod* function is defined by

$$(3.16) \quad MM\left(L_{\mathcal{M}} f(x)\right) = \begin{cases} \min_{m \in \mathcal{M}} L_m f(x) & \text{if } L_m f(x) > 0 \text{ for all } m \in \mathcal{M}, \\ \max_{m \in \mathcal{M}} L_m f(x) & \text{if } L_m f(x) < 0 \text{ for all } m \in \mathcal{M}, \\ 0 & \text{otherwise.} \end{cases}$$

Theorem 3.4 characterizes the convergence of the *minmod* function applied to the set of edge detectors  $L_m f$  of various order  $m$  and demonstrates its ability to distinguish jump discontinuities from neighborhood oscillations.

THEOREM 3.4. If  $\mathcal{M} = \{1, 2, \dots, \mu\}$ , we have

$$MM\left(L_{\mathcal{M}} f(x)\right) = \begin{cases} [f](\xi) + \mathcal{O}(h(x)) & \text{if } x_{j-1} \leq \xi, x \leq x_j, \\ \mathcal{O}(h^{\min(\mathcal{M}_x, k)}(x)) & \text{if } f \in C^k(I_x), \end{cases}$$

where  $I_x$  is the smallest closed interval such that  $\mathcal{S}_x \subset I_x$  with  $\#\mathcal{S}_x \leq \binom{\mathcal{M}_x+1}{1}$ , and  $\mathcal{M}_x$  is defined by

$$(3.17) \quad \mathcal{M}_x := \max \{m \in \mathcal{M} \mid \#\mathcal{S}_x = m_1, I_x \cap J = \emptyset\}.$$

*Proof.* For  $x \in [a, b]$ , assume without loss of generality that  $x_{j-1} \leq x \leq x_j$  for some  $x_{j-1}, x_j \in \mathcal{S}$ . If there exists  $\xi \in J$  such that  $x_{j-1} \leq \xi \leq x_j$ , then by Theorem 3.1 we have

$$L_m f(x) = [f](\xi) + \mathcal{O}(h(x))$$

for any  $m \in \mathcal{M}$ . Therefore, it is possible to conclude that

$$MM(L_{\mathcal{M}} f(x)) = [f](\xi) + \mathcal{O}(h(x)).$$

If  $J \cap [x_{j-1}, x_j] = \emptyset$ , then by definition we have  $\mathcal{M}_x \geq 1$ . Also from the definition of  $\mathcal{M}_x$ , for any  $m \in \mathcal{M}$  such that  $m \leq \mathcal{M}_x$  and  $\#\mathcal{S}_x = m_1$  we have  $I_x \cap J = \emptyset$ . Therefore, Theorem 3.1 implies that  $L_m f(x) = \mathcal{O}(h^{\min(m,k)}(x))$ , yielding

$$MM(L_{\mathcal{M}} f(x)) = \mathcal{O}(h^{\min(\mathcal{M}_x,k)}(x))$$

to complete the proof.  $\square$

By including  $1 \in \mathcal{M}$  in Theorem 3.4, first order convergence is ensured at edges, even in the case where edges are in neighboring centers. Large values are also included in the set  $\mathcal{M}$  so that there will be a high order of convergence away from the discontinuity.

The *minmod* edge detection method relaxes the assumption for edge resolution in Theorem 3.1, specifically that edge detection is possible only if a maximum of one edge is contained in each local set, or equivalently

$$(3.18) \quad \#([x_j, x_{j+m_1}] \cap J) \leq 1 \quad \text{for } j = 1, \dots, N - m_1,$$

where  $J$  is the set of discontinuities of  $f$  on  $[a, b]$ . In this case, only a certain density of edges can be resolved, i.e., only one discontinuity can be resolved for each  $m_1$  points. Furthermore, the order of the method is restricted to the “closeness” of the edges in terms of their grid point location. Theorem 3.4 relaxes this assumption so that edge resolution is possible if  $J$ , the set of discontinuities of  $f$  on  $[a, b]$ , satisfies

$$(3.19) \quad \#([x_j, x_{j+1}] \cap J) \leq 1 \quad \text{for } j = 1, \dots, N - 1,$$

i.e., the edges can occur at neighboring grid point values. If this requirement is not satisfied, the problem is clearly underresolved.

The superior convergence properties of the *minmod* edge detection method for Example 3.1 with  $\mathcal{M} = \{1, 2, \dots, 6\}$  are evident in Figure 3.3. Of particular interest is the ability of the *minmod* edge detection method to resolve the local jump function even when the first order approximation, as displayed in Figure 3.2(a), detects edges in smooth regions that are artifacts of the variability of the function and sparse sampling. Residual small oscillations that are still evident can be removed by a thresholding process.

The algorithm in Appendix A details the one-dimensional edge detection computation of Examples 3.1, where the particular choice of local sets, reconstruction grid points, and basis functions are specified.

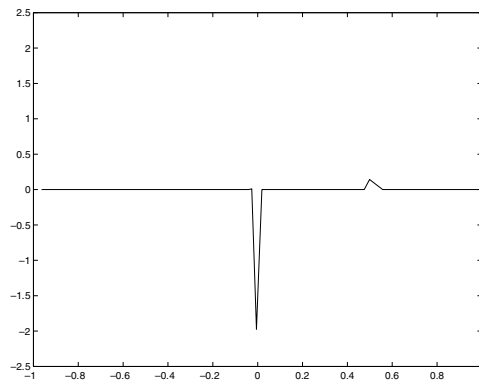


FIG. 3.3. The minmod edge detection method,  $MM(L_{\mathcal{M}}f(x))$ , for Example 3.1. Here  $\mathcal{M} = \{1, 2, \dots, 6\}$ .

#### 4. Edge detection in two dimensions.

**4.1. Formulation.** Throughout section 4, let  $f$  be a piecewise smooth function on a domain  $\Omega \subset \mathbb{R}^2$  known only on the set of discrete nodes

$$\mathcal{S} \subset \Omega, \quad \#\mathcal{S} =: N < \infty.$$

Though  $d$  indicates an arbitrary dimension, here we consider only the bivariate case. The higher-dimensional case can be similarly constructed with more complicated numerical algorithms.

In two dimensions a jump discontinuity at  $x = \xi$  is identified by its enclosed points (i.e., triangular points) and is characterized by the convergence property away from the discontinuities. Specifically, the enclosed points can be defined by the Delaunay triangulation for  $\mathcal{S}$  that consists of the set of lines connecting each point to its natural neighbors [10]. These sets of lines form elementary triangles whose vertices consist of points in  $\mathcal{S}$ . A triangle is considered elementary if every combination of vertex pairs are natural neighbors. Let the number of elementary triangles of the set  $\mathcal{S}$  be defined as  $N_T$ . We denote the set of vertices of all elementary triangles in the Delaunay triangulation of  $\mathcal{S}$  as

$$(4.1) \quad \mathcal{T}_{\mathcal{S}} = \left\{ T_j \mid T_j := \{x_1^j, x_2^j, x_3^j\} \subset \mathcal{S} \text{ for } j = 1, \dots, N_T \right\},$$

where  $T_j$  is the set of vertices for an elementary triangle.

Since discontinuities are identified at specific points by their enclosed cells, the local sets  $\mathcal{S}_x$  are chosen to include points that characterize these cells. For arbitrary  $x \in \Omega$ , we can assume without loss of generality that  $x \in K_{T_j} \subset \Omega$ . Recall that  $K_{T_j}$  is the convex hull of the set of vertices  $T_j \in \mathcal{T}_{\mathcal{S}}$ . Therefore the local set  $\mathcal{S}_x$  for arbitrary  $x \in \Omega$  can now be defined specifically to include the set that characterizes its enclosed points as

$$(4.2) \quad \mathcal{S}_x := T_j \cup \mathcal{S}_{T_j},$$

where  $T_j \in \mathcal{T}_{\mathcal{S}}$ ,  $x \in K_{T_j}$ , and  $\mathcal{S}_{T_j}$  is the set of the  $m_2 - 3$  closest points to  $x$  in the set  $\mathcal{S} \setminus T_j$ . To illustrate how  $\mathcal{S}_x$  is chosen, Figure 4.1 depicts a region of the Delaunay

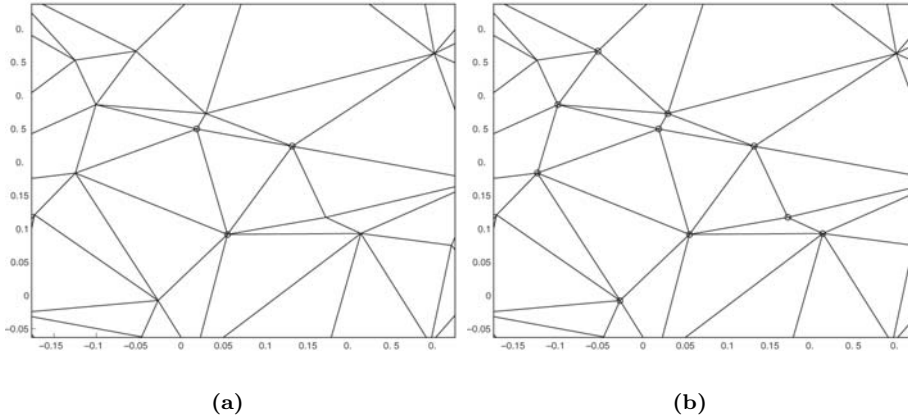


FIG. 4.1. A region of the Delaunay triangulation of 256 randomly sampled points on  $[-1, 1] \times [-1, 1]$ . (The region is enlarged for visibility purposes.) (a) The elementary triangle  $T_j$  that satisfies  $x \in K_{T_j}$ , represented by circles. (b) Pictorial representation of the local set  $\mathcal{S}_x := T_j \cup \mathcal{S}_{T_j}$ , where  $\#\mathcal{S}_x = 10$ .

triangulation of 256 randomly sampled points on  $[-1, 1] \times [-1, 1]$ . Figure 4.1(a) displays a point  $x$  and the elementary triangle  $T_j$  that satisfies  $x \in K_{T_j}$ . Figure 4.1(b) exhibits a local set  $\mathcal{S}_x$  as defined in (4.2), where  $\#\mathcal{S}_x = 10$ .

In order to quantify the convergence rate of the edge detection method, we define

$$(4.3) \quad h(x) := \max_{x \in K_{\mathcal{S}_x}} \min_{x_j \in \mathcal{S}_x} |x - x_j|,$$

which is dependent upon the density of the local set  $\mathcal{S}_x$ .

Recall that for a given positive integer  $m$ , the dimension of  $\Pi_m$  in  $\mathbb{R}^2$  is denoted by  $m_2$  (2.1). If  $\mathcal{S}_x$  is a local set of  $m_2$  points around  $x$ , the function  $L_m f$  is given by

$$(4.4) \quad L_m f(x) = \frac{1}{q_{m,2}(x)} \sum_{x_j \in \mathcal{S}_x} c_j(x) f(x_j),$$

where the coefficients  $c_j(x)$ ,  $j = 1, \dots, m_2$ , are dependent upon the local set  $\mathcal{S}_x$  and satisfy the linear system

$$(4.5) \quad \sum_{x_j \in \mathcal{S}_x} c_j(x) p_i(x_j) = \sum_{|\alpha|_1=m} p_i^{(\alpha)}(x), \quad i = 1, \dots, m_2, \quad \alpha \in \mathbb{Z}_+^2.$$

Here  $p_i$ ,  $i = 1, \dots, m_2$ , form a basis of  $\Pi_m$ . Further illustration of the application of (4.5) for a particular basis of  $\Pi_m$  is detailed in Appendix B. It is easy to check that  $c_j(x) = \mathcal{O}(h(x)^{-m})$ , implying that  $q_{m,2}(x) = \mathcal{O}(h(x)^{-m})$  as well. Recall that in the one-dimensional case, the constant  $q_{m,1}$  is used to determine the jump amplitude at a discontinuity. In the bivariate case, the jump amplitude may vary depending on the paths through a given discontinuity, so quantifying the jump amount at such discontinuity points is not meaningful. However, in the case where jump discontinuities arise locally along a simple curve, we can estimate the jump magnitude in the normal direction with a suitable  $q_{m,2}(x)$  and then apply the *minmod* edge detection method from (3.16) to pinpoint the edges. This will be discussed further in section 4.2. For now we limit our discussion to detecting edges without consideration of their jump amounts.

Since  $c_j(x) = \mathcal{O}(h(x)^{-m})$ , it is possible to bound  $L_m f$  uniformly by defining

$$(4.6) \quad q_m(x) = q_{m,2}(x) := \sum_{x_j \in \mathcal{P}_x} c_j(x),$$

where  $\mathcal{P}_x$  can be a suitable subset of  $\mathcal{S}_x$  such that  $q_m(x) \neq 0$ . This will be discussed later following Definition 4.1, where we will see that the versatility of  $\mathcal{P}_x$  can be utilized to provide a good approximation to the jump magnitudes in the normal directions of the edges in the multivariate case.

Theorem 4.1 establishes the convergence rate of  $L_m f(x)$ , defined in (4.4), away from the discontinuities of  $f$ .

**THEOREM 4.1.** *Suppose  $f$  is a piecewise smooth function on a domain  $\Omega$  in  $\mathbb{R}^2$  known only on discrete nodes  $\mathcal{S}$ . Let  $J$  denote the set of jump discontinuities of  $f$  in  $\Omega$ , and let  $L_m f$  be defined as in (4.4) with  $m \in \mathbb{N}$ . Then if  $f \in C^k(K_{\mathcal{S}_x})$  for some  $k > 0$ , we have*

$$L_m f(x) = \mathcal{O}(h^{\min(k,m)}(x)).$$

*Proof.* The technique of proving Theorem 3.1 is adapted in a straightforward fashion to prove this theorem. Assuming that  $f \in C^k(K_{\mathcal{S}_x})$  for some  $k > 0$ , we define  $k_m := \min(k, m)$  and then separate  $f$  into two parts:

$$f = T_{k_m-1} f + R_{k_m-1} f,$$

where  $T_{k_m-1} f$  is the Taylor polynomial of  $f$  of degree  $(k_m - 1)$  around  $x$ , namely,

$$(4.7) \quad T_{k_m-1} f(y) = \sum_{|\alpha|_1 \leq k_m-1} (y-x)^\alpha D^{(\alpha)} f(x) / \alpha!,$$

and  $R_{k_m-1} f$  is its remainder. Then from the definition of  $c_j(x)$  in (4.5) we see that

$$\sum_{x_j \in \mathcal{S}_x} c_j(x) T_{k_m-1}(x_j) = 0,$$

leading to the relation

$$\begin{aligned} L_m f(x) &= \frac{1}{q_m(x)} \sum_{x_j \in \mathcal{S}_x} c_j(x) R_{k_m-1} f(x_j) \\ &= \frac{1}{q_m(x)} \sum_{x_j \in \mathcal{S}_x} c_j(x) \sum_{|\alpha|_1 = k_m} (x_j - x)^\alpha D^{(\alpha)} f(\zeta_j) / \alpha! \end{aligned}$$

for some  $\zeta_j$  between  $x_j$  and  $x$ . Since  $c_j(x)$  and  $q_m(x)$  are both  $\mathcal{O}(h(x)^{-m})$ , we obtain the relation  $L_m f(x) = \mathcal{O}(h^{k_m}(x))$ , which completes the proof.  $\square$

*Remark 4.1.* As in the univariate case, if the data are given on a uniform grid  $\mathcal{S}$ , we can find a unique set of coefficients  $c_j(x) = c_j$ ,  $j = 1, \dots, m_2$ , with  $m_2$  given in (2.1), and apply it to construct  $L_m f(x)$ , regardless of the position  $x$  (away from the boundary of  $\Omega$ ) and the density  $h(x)$  of points. Let  $\mathbf{U}$  be a set of integers around the origin with  $\#\mathbf{U} = m_2$ , and assume that for any  $x$ , the shape of the stencil of  $\mathcal{S}_x$  is the same as  $\mathbf{U}$ ; i.e., there exists  $\nu(x) \in h\mathbb{Z}^2 \cap \Omega$  such that

$$(4.8) \quad \mathcal{S}_x = \nu(x) + h\mathbf{U}, \quad h > 0.$$

Solving the linear system

$$(4.9) \quad \sum_{j \in \mathbf{U}} c_j \frac{j^\alpha}{\alpha!} = \delta_{m_2, |\alpha|_1}, \quad \alpha \in \mathbb{Z}_+^2, \quad |\alpha|_1 \leq m_2,$$

we define  $L_m f$  as follows:

$$(4.10) \quad L_m f(x) = \frac{1}{q_m} \sum_{j \in \mathbf{U}} c_j f(\nu(x) + jh),$$

where  $q_m$  is also independent of  $x$ . Note that  $c_j$  and  $q_m$  are bounded by a constant, while if  $\mathcal{S}_x$  is a scattered data set, they are  $\mathcal{O}(h^{-m}(x))$ . A straightforward application of the proof in Theorem 4.1 shows that for the uniform case with  $h = h(x)$ , we have

$$L_m f(x) = \mathcal{O}(h^{\min(k,m)}).$$

**4.2. Minmod edge detection in two dimensions.** As in the one-dimensional case, the utilization of the *minmod* edge detection method increases the area of convergence away from the discontinuities of  $f$ . Theorem 4.1 establishes that for a certain order  $m$ , the edge detection method  $L_m f(x)$  defined in (4.4) converges to zero away from the discontinuities if  $K_{\mathcal{S}_x} \cap J = \emptyset$ . Here  $J$  denotes the set of jump discontinuities of  $f$  in  $\Omega$ . Theorem 4.2 demonstrates that the *minmod* edge detection method converges to zero away from the discontinuities if  $K_{T_j} \cap J = \emptyset$ , where  $T_j \in \mathcal{T}_S$  is defined in (4.1). Clearly this is an improvement since  $K_{T_j} \subset K_{\mathcal{S}_x}$ .

**THEOREM 4.2.** *If  $x \in K_{T_j}$  and  $K_{T_j} \cap J = \emptyset$  for some  $T_j \in \mathcal{T}_S$  (4.1), then the minmod edge detection method (3.16) for the set  $\mathcal{M} = \{1, 2, \dots, \mu\}$  has the property*

$$MM(L_{\mathcal{M}} f(x)) = \mathcal{O}(h^{\min(\mathcal{M}_x, k)}(x)),$$

where  $\mathcal{M}_x$  is defined as

$$(4.11) \quad \mathcal{M}_x := \max \{m \in \mathcal{M} : K_{\mathcal{S}_x} \cap J = \emptyset, \#\mathcal{S}_x = m_2\},$$

and  $f \in C^k(K_{\mathcal{S}_x})$  for some  $k > 0$  with  $\#\mathcal{S}_x \leq \binom{\mathcal{M}_x + 2}{2}$ .

*Proof.* Assume that  $x \in K_{T_j}$  and  $K_{T_j} \cap J = \emptyset$  for some  $T_j \in \mathcal{T}_S$ . Since  $K_{T_j} \cap J = \emptyset$  we have  $\mathcal{M}_x \geq 1$ . Then for any  $m \in \mathcal{M}$  such that  $m \leq \mathcal{M}_x$ , the corresponding local set  $\mathcal{S}_x$  such that  $\#\mathcal{S}_x = m_2$  will satisfy  $\mathcal{S}_x \cap J = \emptyset$ . Theorem 4.1 then gives  $L_m f(x) = \mathcal{O}(h^{\min(m, k)}(x))$ . Therefore

$$MM(L_{\mathcal{M}} f(x)) = \mathcal{O}(h^{\min(\mathcal{M}_x, k)}(x)),$$

which finishes the proof.  $\square$

As in the case of one dimension, the choice of  $\mathcal{M}$  in Theorem 4.2, an arbitrary set of positive integers, is purposeful. By including  $1 \in \mathcal{M}$ , first order convergence is ensured at the neighboring cells of discontinuities. Large values are also included in the set  $\mathcal{M}$  so that there will be a high order of convergence away from the discontinuities.

Recall that for any particular point  $x \in \Omega$ , the normalization factor  $q_m(x)$  in (4.6) is defined for a subset  $\mathcal{P}_x \subset \mathcal{S}_x$  such that  $q_m(x) \neq 0$ . Theorem 4.3 demonstrates that for a particular  $\mathcal{P}_x$  the *minmod* edge detection method will provide a good approximation to the jump magnitudes in the normal directions of the edges. To accomplish this approximation, we provide the following definition.

DEFINITION 4.1. For an arbitrary point  $x \in \Omega$  of a piecewise smooth function  $f$ , define the subset  $\mathcal{P}_x$  of the local set  $\mathcal{S}_x \subset \mathcal{S}$  as

$$(4.12) \quad \mathcal{P}_x = \arg \max_{\mathcal{P}} \{ \#\mathcal{P} \mid \mathcal{P} \subset \mathcal{S}_x, \text{ and } f \in C^k(K_{\mathcal{P}}) \text{ for some } k > 0 \}.$$

Therefore  $\mathcal{P}_x$  is the largest subset of the local set  $\mathcal{S}_x$  such that  $f \in C^k(K_{\mathcal{P}_x})$  for some  $k > 0$ . (A technique for approximating this particular  $\mathcal{P}_x$  is provided in Appendix B.)

As in the one-dimensional case,  $q_m(x)$  can be considered as a generalized version of divided difference for the characteristic function  $\chi_{\mathcal{P}_x}$  on  $\mathcal{S}_x$  (see the ‘‘Remark’’ following Theorem 3.2). Hence, the condition  $q_m(x) \neq 0$  is reasonable. Further, it is assumed without loss of generality in the following analysis that for a small enough local set, if  $\mathcal{P}_x \neq \mathcal{S}_x$ , then  $f \in C^k(K_{\mathcal{P}_x^c \cap \mathcal{S}_x})$  for some  $k > 0$ . Here  $\mathcal{P}_x^c$  indicates the complement of the set  $\mathcal{P}_x$ . This assumption is similar to the one-dimensional case, where it is assumed that each local set contains at most one discontinuity. If this assumption is not true, the problem is clearly underresolved.

Theorem 4.3 characterizes the *minmod* edge detection method for the two-dimensional edge detection function  $|L_m f|$  in (4.4). In this case, we use the absolute value of (4.4) since the jump amplitude may vary depending on paths through a given discontinuity.

THEOREM 4.3. For each  $m \in \mathbb{N}$ , define  $L_m f$  as in (4.4) with  $q_m(x)$  given in (4.6). If  $x \in K_{T_j}$  for some  $T_j \in \mathcal{T}_{\mathcal{S}}$ , then the *minmod* edge detection method (3.16) for the set  $\mathcal{M} = \{1, 2, \dots, \mu\}$  has the property

$$MM(|L_{\mathcal{M}} f(x)|) = \begin{cases} [F](x) + \mathcal{O}(h(x)) & \text{if } K_{T_j} \cap J \neq \emptyset, \\ \mathcal{O}(h^{\min(\mathcal{M}_x, k)}(x)) & \text{if } K_{T_j} \cap J = \emptyset, \end{cases}$$

where  $\mathcal{M}_x$  is defined in (4.11),  $f \in C^k(K_{\mathcal{S}_x})$  for some  $k > 0$  with  $\#\mathcal{S}_x \leq \binom{\mathcal{M}_x+2}{2}$ , and

$$(4.13) \quad [F](x) := \max \{ |f(u) - f(v)| : u \in K_{\mathcal{P}_x} \cap K_{T_j}, v \in K_{\mathcal{P}_x^c \cap \mathcal{S}_x} \cap K_{T_j} \}.$$

*Proof.* For any given integer  $m \in \mathcal{M}$ , choose the local set  $\mathcal{S}_x$  such that  $\#\mathcal{S}_x = m_2$ . Assume first  $K_{T_j} \cap J \neq \emptyset$ . Then clearly  $\mathcal{P}_x, \mathcal{P}_x^c \cap \mathcal{S}_x \neq \emptyset$ . Now, for some  $\beta_j, \gamma_j \in (0, 1)$ , we have

$$\begin{aligned} |L_m f(x)| &= \left| \frac{1}{q_m(x)} \sum_{x_j \in \mathcal{P}_x} c_j(x) f(x_j) + \frac{1}{q_m(x)} \sum_{x_j \in \mathcal{P}_x^c \cap \mathcal{S}_x} c_j(x) f(x_j) \right| \\ &= \left| \frac{1}{q_m(x)} \sum_{x_j \in \mathcal{P}_x} c_j(x) \left[ f(u) + \sum_{|\alpha|_1=1} (x_j - u)^\alpha D^\alpha f(u + \beta_j(x_j - u)) \right] \right. \\ &\quad \left. + \frac{1}{q_m(x)} \sum_{x_j \in \mathcal{P}_x^c \cap \mathcal{S}_x} c_j(x) \left[ f(v) + \sum_{|\alpha|_1=1} (x_j - v)^\alpha D^\alpha f(v + \beta_j(x_j - u)) \right] \right| \end{aligned}$$

for any  $u \in K_{\mathcal{P}_x} \cap K_{T_j}$  and  $v \in K_{\mathcal{P}_x^c \cap \mathcal{S}_x} \cap K_{T_j}$ . From the condition  $\sum_{j \in \mathcal{S}_x} c_j(x) = 0$ , we see from (4.6) that

$$q_m(x) = \sum_{x_j \in \mathcal{P}_x} c_j(x) = - \sum_{x_j \in \mathcal{P}_x^c \cap \mathcal{S}_x} c_j(x),$$

and therefore

$$|L_m f(x)| = |f(u) - f(v)| + \mathcal{O}(h(x)).$$



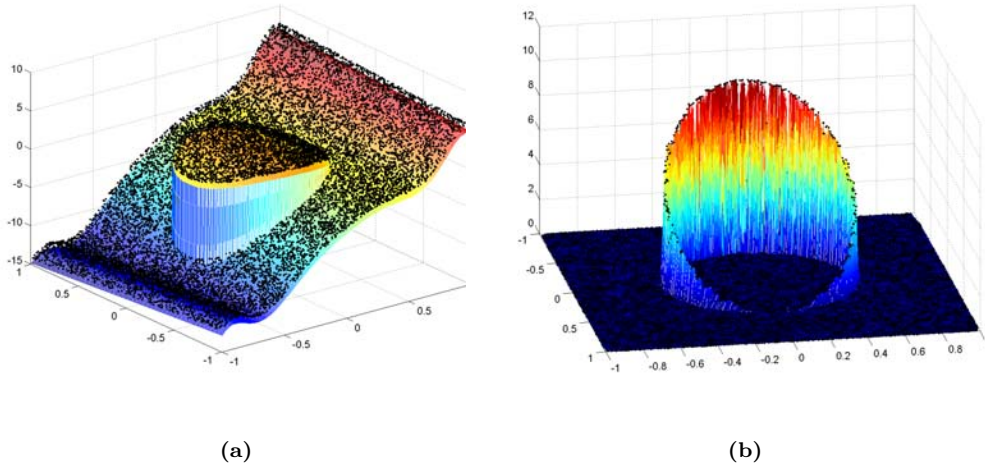


FIG. 4.2. (a)  $f_1(x)$  from Example 4.1 sampled on random points with  $\#\mathcal{S} = 128^2$ . (b) The *minmod* edge detection method of  $MM(L_{\mathcal{M}}f_1(x))$  for  $\mathcal{M} = \{1, 2, 3, 4\}$ .

Since  $u$  and  $v$  are arbitrary points in the sets  $K_{\mathcal{P}_x} \cap K_{T_j}$  and  $K_{\mathcal{P}_x \cap \mathcal{S}_x} \cap K_{T_j}$ , respectively, we obtain that  $|L_m f(x)| = [F](x) + \mathcal{O}(h(x))$ , where  $[F](x)$  is defined in (4.13), yielding

$$MM(|L_{\mathcal{M}}f(x)|) = [F](x) + \mathcal{O}(h(x)).$$

Next, assume that  $K_{T_j} \cap J = \emptyset$ . By definition,  $\mathcal{M}_x \geq 1$ . Then for any  $m \in \mathcal{M}$  such that  $m \leq \mathcal{M}_x$ , the corresponding local set  $\mathcal{S}_x$  such that  $\#\mathcal{S}_x = m_2$  will satisfy  $\mathcal{S}_x \cap J = \emptyset$ . Theorem 4.1 then gives  $L_m f(x) = \mathcal{O}(h^{\min(m,k)}(x))$ . Clearly it can be concluded that

$$MM(|L_{\mathcal{M}}f(x)|) = \mathcal{O}(h^{\min(\mathcal{M}_x,k)}(x)),$$

which finishes the proof.  $\square$

To demonstrate the efficacy of the *minmod* edge detection method in two dimensions we consider the following example.

Example 4.1.

$$f_1(x) := f_1(u, v) := \begin{cases} uv + \cos(2\pi u^2) - \sin(2\pi u^2) & \text{if } u^2 + v^2 \leq \frac{1}{4}, \\ 10u - 5 + uv + \cos(2\pi u^2) - \sin(2\pi u^2) & \text{if } u^2 + v^2 > \frac{1}{4} \end{cases}$$

for  $-1 \leq u, v \leq 1$ .

Note that the edges comprise the circle  $u^2 + v^2 = \frac{1}{4}$  with the exception of  $u = \frac{1}{2}$ , where the function is smooth. Figure 4.2(a) shows  $f_1(x)$  sampled on a MATLAB randomly generated data set  $\mathcal{S}$  with  $\#\mathcal{S} = 128^2$ . Figure 4.2(b) displays the results of applying the *minmod* edge detection method to  $L_m f_1$  with  $m \in \mathcal{M} = \{1, 2, 3, 4\}$ . Of particular interest is the ability of the *minmod* edge detection method to resolve the positions and magnitudes in the normal direction of the edges even in areas of sparse sampling and steep gradients.

Let us now turn our attention to a practical example often used as a benchmark test for edge detection in magnetic resonance imaging (MRI).

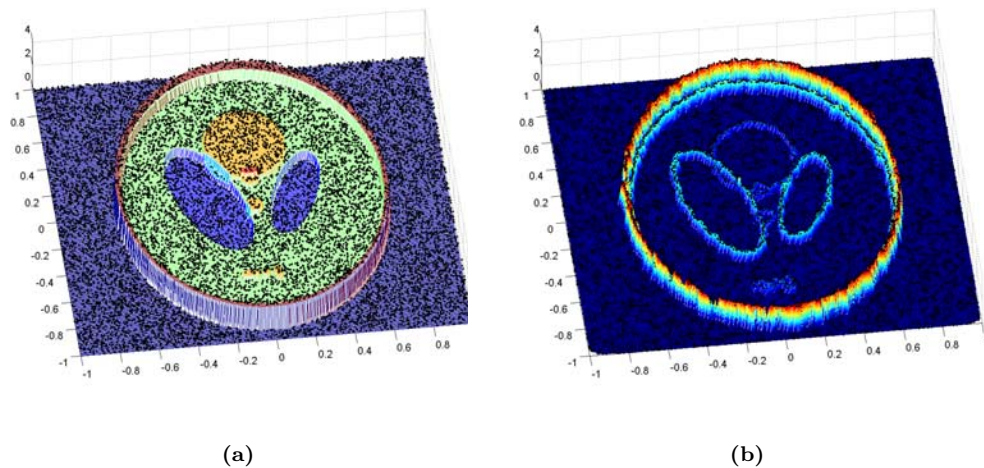


FIG. 4.3. (a)  $f_2(x)$  from Example 4.2 sampled on random points with  $\#\mathcal{S} = 128^2$ . (b) The *minmod* edge detection method of  $MM(L_{\mathcal{M}}f_2(x))$  for  $\mathcal{M} = \{1, 2, 3, 4\}$ .

*Example 4.2.* The so-called Shepp–Logan phantom,  $f_2(x)$ , defined in Appendix C.

Note that the edges of the Shepp–Logan phantom comprise various ellipses of different sizes and orientations, some of which overlap. Figure 4.3(a) shows the Shepp–Logan phantom (denoted as  $f_2(x)$ ), sampled on a MATLAB randomly generated data set  $\mathcal{S}$  with  $\#\mathcal{S} = 128^2$ . Figure 4.3(b) displays the results of applying the *minmod* edge detection method on  $L_m f_2(x)$  with  $m \in \mathcal{M} = \{1, 2, 3, 4\}$ . Of particular interest is the ability of the *minmod* edge detection method to resolve edges that reside in neighboring centers.

The algorithm in Appendix B details the two-dimensional edge detection computation for Examples 4.1 and 4.2, where the particular choice of local sets, reconstruction points, and basis functions are specified. Although no formal computational cost studies were conducted, our experiments indicate that the two-dimensional algorithm experiences minimal increase in computational effort.

**5. Concluding remarks.** In this paper we have introduced an edge detection method (2.5) based on a local polynomial annihilation property on a set of irregularly distributed points in a bounded domain  $\Omega \subset \mathbb{R}^d$ . The method successfully captures discontinuities that are identified by their enclosed cells by characterizing the convergence away from the discontinuities. Although the convergence of the edge detection method can be of high order away from discontinuities, there are problematic oscillations in the neighborhoods of discontinuities. The *minmod* function (3.6) for one-dimensional global edge detection methods enables the distinction of jump discontinuities from neighborhood oscillations by the effective use of the information intrinsic to the edge detection approximation. The resulting *minmod* edge detection method ensures the highest rate of convergence *up to* the enclosed points of discontinuities.

The edge detection method described in our study is local, numerically cost efficient, and entirely independent of any specific shape or complexity of boundaries. Furthermore, it demonstrates the ability to detect edges of piecewise smooth functions with steep gradients as well as in low resolution environments with sparse, nonuniform

sampling. For uniformly distributed points, the cost of computation is significantly reduced since the coefficients in the edge detection method are constant for every type of local stencil.

This study is concerned with the detection of jump discontinuities. Our future work will focus on integrating this method to real signals and images in various scientific disciplines, where noise, poor resolution, and numerical efficiency all become critical issues. We also are currently generalizing our method to determine jump discontinuities in the derivatives, critical for resolving texture in images.

**Appendix A. One-dimensional edge detection algorithm.** For any  $x \in [a, b]$ , let  $\mathcal{S}_x$  be the closest  $m_1 = m + 1$  points to  $x$  in  $\mathcal{S}$ . As a basis of  $\Pi_m$ , choose  $p_i(x) = x^{i-1}$  for  $i = 1, \dots, m_1$ . The *minmod* function for  $\mathcal{M} = \{1, 2, \dots, \mu\}$  will be reconstructed on the points  $x_{j+\frac{1}{2}} = \frac{1}{2}(x_{j+1} + x_j)$  with  $j = 1, \dots, N - 1$ .

**for**  $m = 1$  to  $\mu$  and  $j = 1$  to  $N - 1$

**step 1.** For each  $x_{j+\frac{1}{2}}$ , define  $\mathcal{S}_{x_{j+\frac{1}{2}}}^+ = \{x_n | x_n > x_{j+\frac{1}{2}}\}$  and set  $r = \#\mathcal{S}_{x_{j+\frac{1}{2}}}^+$ .

**step 2.** Calculate the coefficients

$$c_i(x_{j+\frac{1}{2}}) = \frac{m!}{\omega_i(\mathcal{S}_{x_{j+\frac{1}{2}}})}, \quad i = 1, \dots, m_1,$$

where  $\omega_i(\mathcal{S}_{x_{j+\frac{1}{2}}})$  is defined as in (3.9).

**step 3.** Calculate the normalization factor

$$q_m(x_{j+\frac{1}{2}}) = \sum_{i=m_1-r+1}^{m_1} c_i(x_{j+\frac{1}{2}}).$$

**step 4.** Compute the jump function

$$L_m f(x_{j+\frac{1}{2}}) = \frac{1}{q_m(x_{j+\frac{1}{2}})} \sum_{i=1}^{m_1} c_i(x_{j+\frac{1}{2}}) f(x_{i+j+r-m_1}).$$

**end** ( $m, j$ )

**step 5.** Apply *minmod* edge detection method  $MM(L_{\mathcal{M}}f(x_{j+\frac{1}{2}}))$ .

**Appendix B. Two-dimensional edge detection algorithm.** Let  $\mathcal{S} := \{x_j := (u_j, v_j) | j = 1, \dots, N\} \subset \Omega$  and choose  $p_\alpha(x) = u^{\alpha_1} v^{\alpha_2}$  for  $x = (u, v)$  and  $\alpha = (\alpha_1, \alpha_2) \in \mathbb{Z}_+^2$  such that  $|\alpha|_1 \leq m$  as a basis of  $\Pi_m$ . The *minmod* function for  $\mathcal{M} = \{1, 2, \dots, \mu\}$  will be reconstructed on the set

$$(B.1) \quad \mathcal{D}_{\mathcal{T}_S} = \left\{ \bar{x}_j \mid \bar{x}_j = \frac{\sum_{i=1}^3 x_i^j}{3}, \text{ where } T_j = \{x_1^j, x_2^j, x_3^j\} \in \mathcal{T}_S \text{ for } j = 1, \dots, N_T \right\}.$$

**for**  $m = 1$  to  $\mu$  and  $j = 1$  to  $N_T$

**step 1.** For  $\bar{x}_j$  in (B.1), determine  $\mathcal{S}_{\bar{x}_j}$  as in (4.2) with  $\#\mathcal{S}_{\bar{x}_j} = m_2 = \binom{m+2}{2}$ .

Set  $\mathcal{S}_{\bar{x}_j} = \{x_1, \dots, x_{m_2}\}$  such that  $f(x_1) \leq f(x_2) \leq \dots \leq f(x_{m_2})$ .

**step 2.** Solve the linear system

$$\sum_{x_i \in \mathcal{S}_{\bar{x}_j}} c_i(\bar{x}_j) p_\alpha(x_i) = \begin{cases} 0 & \text{if } \alpha_1 + \alpha_2 < m, \\ \alpha_1! \alpha_2! & \text{if } \alpha_1 + \alpha_2 = m \end{cases}$$

for  $\alpha_1, \alpha_2 = 0, \dots, m$ , such that  $\alpha_1 + \alpha_2 \leq m$ .

**step 3.** Calculate  $q_m(\bar{x}_j)$  as in (4.6). Here the subset  $\mathcal{P}_x$  (4.12) of  $\mathcal{S}_{\bar{x}_j}$  is computed as

$$\mathcal{P}_x = \{x_1, \dots, x_r\},$$

where

$$|f(x_{r+1}) - f(x_r)| = \max_{i=1, \dots, m_2-1} |f(x_{i+1}) - f(x_i)|.$$

If such  $r$  is not unique, choose the smallest one.

**step 4.** Calculate  $L_m f(\bar{x}_j) = \frac{1}{q_m(\bar{x}_j)} \sum_{x_i \in \mathcal{S}_{\bar{x}_j}} c_i(\bar{x}_j) f(x_i)$ .

**end** ( $m, j$ )

**step 5.** Apply *minmod* edge detection method  $MM(L_{\mathcal{M}} f(\bar{x}_j))$ .

**Appendix C. Shepp–Logan phantom algorithm.** The Shepp–Logan phantom is a piecewise smooth function on the domain  $\Omega = [-1, 1] \times [-1, 1]$  in  $\mathbb{R}^2$ . For any arbitrary point  $(u, v) \in \Omega$  the value of the Shepp–Logan phantom  $z = f(u, v)$  is calculated as follows:

**for** each point  $(u, v)$

**let**  $z = 0$ ,  $\xi_1 = (u - .22) \cos(.4\pi) + v \sin(.4\pi)$ ,  $\eta_1 = -(u - .22) \sin(.4\pi) + v \cos(.4\pi)$ ,  $\xi_2 = (u + .22) \cos(.6\pi) + v \sin(.6\pi)$ , and  $\eta_2 = -(u + .22) \sin(.6\pi) + v \cos(.6\pi)$ .

**if**  $(\frac{u}{.69})^2 + (\frac{v}{.92})^2 \leq 1$ ,

**then**  $z = 2$ .

**if**  $(\frac{u}{.06624})^2 + (\frac{v+.0184}{.874})^2 \leq 1$ ,

**then**  $z = z - .98$ .

**if**  $(\frac{\xi_1}{.31})^2 + (\frac{\eta_1}{.11})^2 \leq 1$  or  $(\frac{\xi_2}{.41})^2 + (\frac{\eta_2}{.16})^2 \leq 1$ ,

**then**  $z = z - .02$ .

**if**  $(\frac{u-.35}{.3})^2 + (\frac{v}{.6})^2 \leq 1$ , or  $(\frac{u}{.21})^2 + (\frac{v-.35}{.25})^2 \leq 1$ , or  $(\frac{u}{.046})^2 + (\frac{v-.1}{.046})^2 \leq 1$ , or  $(\frac{u}{.046})^2 + (\frac{v+.1}{.046})^2 \leq 1$ , or  $(\frac{u+.08}{.046})^2 + (\frac{v+.605}{.023})^2 \leq 1$ , or  $(\frac{u}{.023})^2 + (\frac{v+.605}{.023})^2 \leq 1$ , or  $(\frac{u-.06}{.023})^2 + (\frac{v+.605}{.023})^2 \leq 1$ ,

**then**  $z = z + .01$ .

**end.**

#### REFERENCES

- [1] R. ABGRALL, *On essentially non-oscillatory schemes on unstructured meshes: Analysis and implementation*, J. Comput. Phys., 114 (1994), pp. 45–54.
- [2] J. CANNY, *A computational approach to edge detection*, IEEE Trans. Pattern Anal. Machine Intell., 8 (1986), pp. 679–698.
- [3] A. GELB AND E. TADMOR, *Detection of edges in spectral data*, Appl. Comput. Harmon. Anal., 7 (1999), pp. 101–135.
- [4] A. GELB AND E. TADMOR, *Detection of edges in spectral data II. Nonlinear enhancement*, SIAM J. Numer. Anal., 38 (2000), pp. 1389–1408.
- [5] M. GÖKMEN AND A. JAIN,  *$\lambda\tau$ -space representation of images and generalized edge detector*, IEEE Trans. Pattern Anal. Machine Intell., 19 (1997), pp. 545–563.
- [6] A. HARTEN, B. ENGQUIST, S. OSHER, AND S. CHAKARVARTHY, *Uniformly high order essentially non-oscillatory schemes*, III, J. Comput. Phys., 71 (1987), pp. 231–303.
- [7] R. J. LEVEQUE, *Finite Volume Methods for Hyperbolic Problems*, Cambridge University Texts, Cambridge, UK, 2002.
- [8] Z.-P. LIANG AND P. C. LAUTERBUR, *Principles of Magnetic Resonance Imaging: A Signal Processing Perspective*, IEEE Press, New York, 2000, pp. 241–243.

- [9] X.-D. LIU, S. OSHER, AND T. CHAN, *Weighted essentially non-oscillatory schemes*, J. Comput. Phys., 115 (1994), pp. 200–212.
- [10] F. P. PREPARATA AND M. I. SHAMOS, *Computational Geometry: An Introduction*, Springer-Verlag, New York, 1985.
- [11] S. MALLAT AND W. HWANG, *Singularity detection and processing with wavelets*, IEEE Trans. Inform. Theory, 38 (1992), pp. 617–643.
- [12] C.-W. SHU, *Essentially Non-oscillatory and Weighted Essentially Non-oscillatory Schemes for Hyperbolic Conservation Laws*, NASA CR-97-206253 ICASE Report 97-65, 1997.
- [13] E. TADMOR, *Private communication*, 2003.
- [14] E. T. WHITTAKER AND G. ROBINSON, *The Calculus of Observation: A Treatise on Numerical Mathematics*, 4th ed., Dover, New York, 1967.
- [15] Y.-T. ZHANG AND C.-W. SHU, *High-order WENO schemes for Hamilton–Jacobi equations on triangular meshes*, SIAM J. Sci. Comput., 24 (2003), pp. 1005–1030.